Mechanically Induced Helicity in Chiral Stimuli-Responsive Gels

Masatoshi Toda*,† and Fumihiko Tanaka

Department of Polymer Chemistry, Graduate School of Engineering, Kyoto University, Katsura, Kyoto 615-8510, Japan

Received March 30, 2007; Revised Manuscript Received April 26, 2007

ABSTRACT: Mechanical and optical responses of chiral stimuli-responsive gels to macroscopic deformation are theoretically studied. We propose a simple elasticity model for the network of helical polymer chains by combining a statistical theory of a single polymer chain bearing induced helices recently presented by us [*Macromolecules* **2005**, *38*, 561] with the classical affine network theory. We find that the stress−strain relation of the network in a solution of chiral molecules has characteristic profiles different from sigmoidal ones observed in the conventional rubberlike materials. We also find that, as the network is uniaxially elongated or compressed, the chirality order parameter, which is proportional to the intensity of circular dichroism of the network, is enhanced in the intermediate region of elongation under certain conditions. Finally, we discuss the possibility of optical resolution of almost racemic mixtures of chiral molecules by using such networks.

1. Introduction

Stereoregular polymers capable of hydrogen-bonding chiral molecules have been recently reported by Yashima et al.[1−3] These polymers themselves do not have chiral centers and are optically inactive in solutions without chiral molecules. When the chiral molecules, such as amines and amino alcohols, are hydrogen-bonded onto side groups of the polymers, helical secondary structures are induced on the polymer, and then the whole polymer becomes optically active. The handedness of the helices is determined by the chirality of the adsorbed molecules. These polymers are called induced-helical polymers. For example, poly(phenylacetylene) derivatives such as poly((4-carboxyphenyl)acetylene) and poly(4-(*N*,*N*-diisopropylaminomethyl)phenylacetylene) fall into this category.

By measuring induced circular dichroism (ICD) spectroscopy in detail, Yashima et al. furthermore found that the following characteristic rules generally hold for solutions of induced-helical polymers:

(1) Nonlinear Amplification. Under the presence of either (*S*)- or (*R*)-form of chiral molecules, the relationship between the optical activity and the concentration of chiral molecules shows sigmoidal profiles. There is a sharp rise of the optical activity due to induced helices in very narrow concentration range of chiral molecules.

(2) Majority Rule. Under the presence of both (*S*)- and (*R*)-forms of chiral molecules, the chirality of the whole system is predominantly determined by the major component of chiral molecules.

(3) Sergeant−Soldiers Rule. Under the presence of a small number of chiral molecules of only one type, achiral molecules act as if they had the same chirality as the chiral molecules. This phenomenon is similar to the situation that many soldiers follow an order of a sergeant simultaneously.

From the theoretical viewpoint, Tanaka[4] and D'Orsogna and Chou[5] have independently succeeded in giving molecular interpretations to some of the rules by mapping the system onto one-dimensional Ising models with nearest-neighbor interactions. These rules are very interesting because there is a possibility of both fundamental and technological applications such as enantioselective catalyses, chirality detectors, and memory elements.

In our previous paper,[6] we theoretically studied the effect of stretching such single helical polymer in a solution of chiral molecules on the basis of standard equilibrium statistical mechanics. In the presence of either (*S*)- or (*R*)-form of chiral molecules, it was found that the force−extension curve shows an anomalous profile different from that of the random flight chain and that the helix content of the polymer increases transiently as the polymer is stretched. Furthermore, we discussed the possibility of optical resolution by stretching such helical polymer in a solution of an almost racemic mixture of chiral molecules.

Recent progress in experimental techniques such as magnetic trap and optical tweezer methods[7,8] enables us to perform single-molecule manipulation on various polymers. These experiments probably reveal force−extension curves of induced-helical polymers. By comparing such experimental data with our numerical results, we can verify whether our model for a single induced-helical polymer is valid or not. In contrast, the helix content of a single polymer cannot be detected by optical measurements such as ICD spectroscopy. The detection of the optical activity by these experiments is effective only for the system containing 10^{23} order of molecules, e.g., solution and film. In order to determine the relationship between the helix content and the end-to-end distance, we need to prepare a system in which we are able to control the end-to-end distance of 10^{23} order of polymers simultaneously.

A network (gel) made by cross-linking induced-helical polymers covalently can fulfill the requirement mentioned above. Macroscopic deformation of the network leads to simultaneous control of the end-to-end distance of 10^{23} order of constituent chains. In addition, the optical activity of the network can be detected experimentally if the network is transparent enough to transmit polarized light. Fortunately, Goto et al. have succeeded in preparing poly((4-carboxyphenyl)-acetylene) gels by cross-linking poly((4-carboxyphenyl)acety-

* To whom correspondence should be addressed. E-mail: toda@cmpt.phys.tohoku.ac.jp.
† Present address: Department of Physics, Tohoku University, Aoba, Aramaki, Aoba-ku, Sendai, 980-8578, Japan.

10.1021/ma070759w CCC: $37.00
Published on Web 06/01/2007

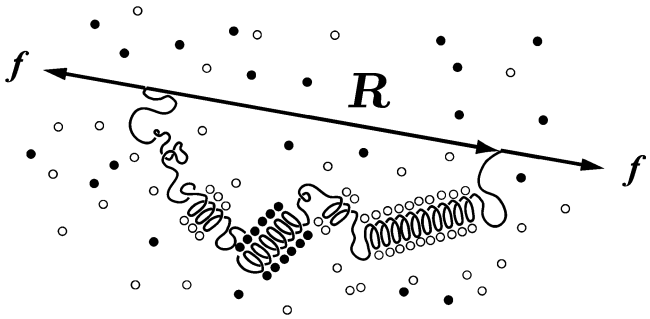

Figure 1. Schematic figure of a single induced-helical polymer with the end-to-end vector $\boldsymbol{R}$ and the tension $\boldsymbol{f}$ exerted at both ends of the chain. The symbols ○ and ● correspond to the chiral molecules in the (*S*)-form and those in the (*R*)-form, respectively.

lene) with diamines.[9] They call such gels chiral stimuli-responsive gels. Thus, our desired system actually exists.

In this paper, we propose a simple model for the network mentioned above by combining the single chain model for the induced-helical polymers[6] with a conventional network theory. We treat only macroscopic uniaxial deformation of the network to investigate both elastic and optical properties of the network. We show that both elongational and compressional deformation of the network in a solution containing chiral molecules can lead to the transient amplification of the optical activity of the network and that the stress−strain relation can have shoulders around the strain states where the optical activity reaches peaks. On the basis of the numerical results about the optical activity, we discuss the possibility of optical resolution by macroscopically deforming such network in a solution of an almost racemic mixture and then propose an example of the procedures for optical resolution.

2. Single Helical Polymer Model

In this section, we review the theoretical model for a single induced-helical polymer with a fixed end-to-end distance. For the details of this model and its numerical results, readers should refer to our previous paper.[6]

2.1. A Helical Polymer with a Fixed End-to-End Distance. Let us consider a single unperturbed random flight chain in a solution containing chiral molecules. The chain is comprised of the total number n of segments. Each bond length between successive segments along the chain is a constant value a. In this study, we treat each segment in the above model chain as a monomeric unit where chiral molecules can be adsorbed pairwise. We assume that when attached onto segments in the chain, the chiral molecules in the (*S*)-form induce left-handed helices on the attached parts while those in the (*R*)-form induce right-handed helices (see Figure 1). In addition, we treat the helices induced on the polymer as rigid rods because the persistence length of the helical parts is usually much greater than that of the coil parts. Let us introduce the normalized length κ of one segment along the axis of the rodlike helix. We assume that the value κ is the same for the helix induced by the chiral molecules in the (*S*)-form and that by the chiral molecules in the (*R*)-form because optically isomeric molecules are chemically and physically the same except for their stereosymmetry and optical properties.

In this section, we first derive the helix content for a single helical polymer. The helix content $\theta^{(\alpha)}$ represents the fraction of segments which belong to the helices induced by the chiral molecules in the type $\alpha = S, R$. Under the condition that the tension $\boldsymbol{f}$ exerted at both ends of the polymer, the activity λ_α of the chiral molecules in the type α, and temperature T are specified, we finally find

$$\theta^{(\alpha)} = \frac{tV_1^{(\alpha)}(\tau,\lambda_\alpha t)}{1 + t\{V_1^{(S)}(\tau,\lambda_S t) + V_1^{(R)}(\tau,\lambda_R t)\}} \tag{1}$$

The new functions $V_k^{(\alpha)}(\tau,x)$ ($k = 0, 1, 2, ...$) are defined as

$$V_k^{(\alpha)}(\tau,x) \equiv \sum_{\zeta=1}^{n} \zeta^k \eta_\zeta^{(\alpha)} \phi_\zeta(\tau) x^\zeta \tag{2}$$

where $\tau \equiv fa/k_BT$ is the dimensionless tension, k_B is Boltzmann's constant, and $\eta_\zeta^{(\alpha)}$ is the statistical weight for an α-type helix with the length ζ (in terms of the number of segments). The functions $\phi_\zeta(\tau)$ in eq 2 are defined as $\phi_\zeta(\tau) \equiv \tilde{g}(\kappa\zeta\tau)/\tilde{g}(\tau)^\zeta$, where $\tilde{g}(\tau) \equiv \sinh \tau/\tau$ is the Laplace transform of the distribution function of the bond between successive segments along the chain without helices. The parameter t is the solution of the following nonlinear equation:

$$\frac{t}{1-t}\{V_0^{(S)}(\tau,\lambda_S t) + V_0^{(R)}(\tau,\lambda_R t)\} = 1 \tag{3}$$

We next derive the force−extension curves for a single helical polymer. The relationship between the average end-to-end distance R and the dimensionless tension τ is finally given in the following form:

$$\frac{R}{na} = \frac{L(\tau) + \kappa t\{W_1^{(S)}(\tau,\lambda_S t) + W_1^{(R)}(\tau,\lambda_R t)\}}{1 + t\{V_1^{(S)}(\tau,\lambda_S t) + V_1^{(R)}(\tau,\lambda_R t)\}} \tag{4}$$

Here, $R/na \equiv l$ is the normalized end-to-end distance. $L(x) \equiv \coth x - 1/x$ is the Langevin function, and the new functions $W_k^{(\alpha)}(\tau,x)$ ($k = 0, 1, 2, ...$) are defined as

$$W_k^{(\alpha)}(\tau,x) \equiv \sum_{\zeta=1}^{n} \zeta^k \eta_\zeta^{(\alpha)} \phi_\zeta(\tau) L(\kappa\zeta\tau) x^\zeta \tag{5}$$

In a series of experiments, the optical activities have been measured as functions of the temperature and the concentrations of the chiral molecules. We here introduce the chirality order parameter ψ defined by the difference of $\theta^{(\alpha)}$

$$\psi \equiv \theta^{(S)} - \theta^{(R)} \tag{6}$$

The parameter ψ is proportional to the optical activities of solutions containing induced-helical polymers as shown in ref 4.

2.2. Statistical Weight of Helices: Zimm−Bragg Model. For further discussion, we have to specify the statistical weight $\eta_\zeta^{(\alpha)}$. In this study, we employ the simplest form proposed by Zimm−Bragg[10,11]

$$\eta_\zeta^{(\alpha)} = \sigma_\alpha u_\alpha(T)^\zeta \tag{7}$$

If the concentrations of the chiral molecules are small, we can assume that each activity is proportional to the molar concentration of the species. Hence, for a dilute solution of the chiral molecules, we can rewrite the product of the activity λ_α and the factor $u_\alpha(T)$ into the form $\lambda_\alpha u_\alpha(T) \equiv \gamma_\alpha \equiv k_\alpha(T)c^{(\alpha)}$, where $c^{(\alpha)}$ is the molar concentration of the chiral molecules in the type α and γ_α is its scaled concentration. $k_\alpha(T)$ is the adsorption equilibrium constant of the molecules in the type α. In what

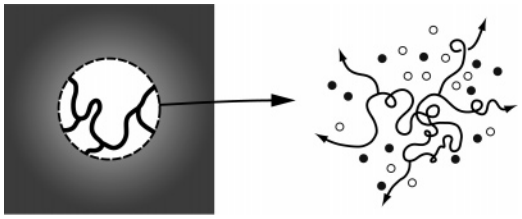

Figure 2. Schematic figure (left) of a chemical gel made by cross-linking induced-helical polymers covalently. In the magnified figure (right), the symbols ○ and ● correspond to the chiral molecules in the (*S*)-form and those in the (*R*)-form, respectively.

follows, we assume that σ_α and $k_\alpha(T)$ are the same for both components, i.e., $\sigma_S = \sigma_R$ and $k_S(T) = k_R(T)$, because optically isomeric molecules have the same properties chemically and physically. We omit the subscript α in σ_α and $k_\alpha(T)$. The factor σ is generally called the helix initiation parameter and is less than 1, which leads to the nonlinear amplification of induced helices as shown in ref 4. We here briefly comment that the parameters σ and $k(T)$ can be evaluated quantitatively by spectrometric measurements such as ICD. For the details, readers should refer to ref 4.

3. Network Model

In this section, by combining the model for a single induced-helical polymer reviewed in the preceding section with a conventional basic network theory originally proposed by Kuhn[12] and later developed by James and Guth[13,14] and others, we construct a model for the chemical gel in which the polymers are cross-linked by covalent bonds (see Figure 2).

3.1. Affine Network Theory. We treat a macroscopic cubic network with a side length L under equilibrium states. For the sake of simplicity, we neglect the chains that do not contribute to the elasticity of the network directly. Then, we assume that all the constituent chains in the network are the chains whose both ends are covalently connected to the different junctions of the network. These chains contribute to the elasticity of the network directly and are called elastically effective chains. Furthermore, the molecular weight distribution of such chains is assumed to be monodispersed with the number n of segments. The elastic free energy of the network deformed with the deformation tensor $\hat{\lambda}$ can be written as follows:

$$F(\hat{\lambda}) = \nu \int \phi(l)\, P(\boldsymbol{l})\, \mathrm{d}\boldsymbol{l} \tag{8}$$

where ν is the total number of constituent chains in the network, $\phi(l)$ is the free energy of a single polymer, and $P(\boldsymbol{l})$ is the probability of finding a constituent chain with its normalized end-to-end vector $\boldsymbol{l}$ in the deformed network. In this study, we employ the following assumptions first introduced by Kuhn.[12] First, we treat the distribution function of each chain in the network before deformation as that of a single polymer chain, $P_0(\boldsymbol{l})$. This assumption is expected to be valid because of the screening effect of the intra- and intermolecular excluded-volume interactions in a dense polymeric system. Second, we introduce the affineness assumption that the microscopic junction sites in the network move affinely with the macroscopic deformation of the network. From these two assumptions, the elastic free energy $F(\hat{\lambda})$ is rewritten as

$$F(\hat{\lambda}) = \nu \int \phi(|\hat{\lambda}\cdot\boldsymbol{l}|) P_0(\boldsymbol{l}) \mathrm{d}\boldsymbol{l} \tag{9}$$

The change in the elastic free energy due to the macroscopic deformation of the network is finally given by

$$\Delta F(\hat{\lambda}) \equiv F(\hat{\lambda}) - F(\hat{1}) = n\nu k_\mathrm{B}T \int [g(|\hat{\lambda}\cdot\boldsymbol{l}|) - g(l)] P_0(\boldsymbol{l})\, \mathrm{d}\boldsymbol{l} \tag{10}$$

where $\hat{1}$ is the unit tensor and the function $g(l)$ is defined as $\phi(l) \equiv nk_\mathrm{B}Tg(l)$.

3.2. Uniaxial Deformation. In order to study basic properties of the network, we impose uniaxial deformation along x-axis on the network as shown in Figure 3. Uniaxial deformation of the network is described by the diagonal deformation tensor

$$\hat{\lambda} \equiv \begin{pmatrix} \lambda_x & 0 & 0 \\ 0 & \lambda_y & 0 \\ 0 & 0 & \lambda_z \end{pmatrix} \tag{11}$$

In this study, we assume that the volume of the system is conserved as in the case of conventional theoretical and simulation studies on rubberlike materials. Hence, the deformation tensor $\hat{\lambda}$ is given in the following simple form: $\lambda_x = \lambda$, $\lambda_y = \lambda_z = 1/\sqrt{\lambda}$. The resilience f_network occurring from the macroscopic deformation of the network is given by the thermodynamic relation $f_\mathrm{network} = (\partial\Delta F/\partial(\lambda L))_T$. By using eq 10 and the normal stress $\sigma_N \equiv f_\mathrm{network}/L^2$, the above relation is rewritten into the stress−strain relation

$$\sigma_N = \frac{n\nu k_\mathrm{B}T}{L^3} \int \frac{\partial g(|\hat{\lambda}\cdot\boldsymbol{l}|)}{\partial\lambda} P_0(\boldsymbol{l})\, \mathrm{d}\boldsymbol{l} \tag{12}$$

In terms of polar coordinates, eq 12 is given in the following form:

$$\sigma_N = \frac{2\pi n\nu k_\mathrm{B}T}{L^3} \int_0^1 \mathrm{d}l\, P_0(\boldsymbol{l}) l^3 \int_0^1 \mathrm{d}\cos\vartheta\, \tau(\eta l) \frac{\mu(\lambda,\vartheta)}{\eta(\lambda,\vartheta)} \tag{13}$$

Here, we treat the dimensionless tension τ as a function of the normalized end-to-end distance l. The function $\eta(\lambda,\vartheta)$ is defined as

$$\eta(\lambda,\vartheta) \equiv \sqrt{\left(\lambda^2 - \frac{1}{\lambda}\right)\cos^2\vartheta + \frac{1}{\lambda}} \tag{14}$$

and the function $\mu(\lambda,\vartheta)$ as

$$\mu(\lambda,\vartheta) \equiv \left(2\lambda + \frac{1}{\lambda^2}\right)\cos^2\vartheta - \frac{1}{\lambda^2} \tag{15}$$

It is both analytically and numerically difficult to perform the multiple integrations in eq 13 because the finite extensibility of each constituent chain in the network results in the divergence of the tension $\tau(l)$ at $l = 1$. In order to avoid such difficulty, we first employ the three-chain approximation originated by James and Guth[13] on the integration over the polar angle ϑ. The three-chain approximation means that elastically effective chains making up the network are replaced by three independent chains pointing toward x-, y-, and z-axes. $\mu/\eta = 2$ and $\eta = \lambda$ in the case of $\vartheta = 0$ (x-axis). Similarly, $\mu/\eta = -\lambda^{-3/2}$ and $\eta = \lambda^{-1/2}$ in the case of $\vartheta = \pi/2$ (y- and z-axes). By using these results, eq 13 is approximately given by

$$\sigma_N \simeq \frac{n\nu k_\mathrm{B}T}{3L^3} \int_0^1 \left[\tau(\lambda l) - \frac{1}{\lambda^{3/2}}\tau\left(\frac{l}{\lambda^{1/2}}\right)\right] 4\pi l^3 P_0(\boldsymbol{l})\, \mathrm{d}l \tag{16}$$

Next, on the integration over the radial coordinate l, we employ the approximation that the radial distribution function $4\pi l^2 P_0(\boldsymbol{l})$ is replaced with $\delta(l - l_\mathrm{av})$. Here, l_av is the root-mean-

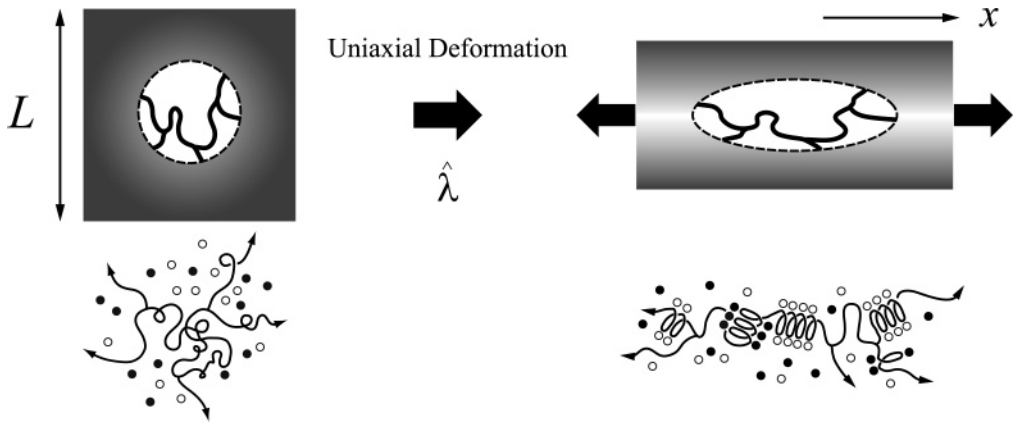

Figure 3. Schematic figure of uniaxial deformation along *x*-axis for the macroscopic cubic network with a side length *L* under equilibrium states. The macroscopic deformation of the network (top). The microscopic deformation of the cross-linked chains in the network (bottom). The symbols ○ and ● correspond to the chiral molecules in the (*S*)-form and those in the (*R*)-form, respectively.

square value $\langle l^2\rangle^{1/2}$ for the distribution function $P_0(\boldsymbol{l})$. In our previous paper,[6] the mean-square end-to-end distance $\langle R^2\rangle_0$ for a induced-helical polymer without conformational constraint was given by

$$\frac{\langle R^2\rangle_0}{na^2} = 1 + \theta_0^{(S)}(\kappa^2\bar{\xi}_{w,0}^{(S)} - 1) + \theta_0^{(R)}(\kappa^2\bar{\xi}_{w,0}^{(R)} - 1) \quad (17)$$

where $\theta_0^{(\alpha)}$ is the α-type helix content at $\tau = 0$ and $\bar{\xi}_{w,0}^{(\alpha)} \equiv V_2^{(\alpha)}(0,\lambda_\alpha t_0)/V_1^{(\alpha)}(0,\lambda_\alpha t_0)$ is the weight-averaged helix length of each chirality on the free polymer. t_0 is the solution of eq 3 at $\tau = 0$. By changing $\langle R^2\rangle_0$ into the form of $l_{av} \equiv \langle R^2\rangle_0^{1/2}/na$ and then performing the approximation, eq 16 is finally given in the following form:

$$\sigma_N \simeq \frac{n\nu k_B T l_{av}}{3L^3}\left\{\tau(\lambda l_{av}) - \frac{1}{\lambda^{3/2}}\tau\left(\frac{l_{av}}{\lambda^{1/2}}\right)\right\} \quad (18)$$

Here, we define the helix content $\theta_{network}^{(\alpha)}(\hat{\lambda})$ and the chirality order parameter $\psi_{network}(\hat{\lambda})$ for a network system by using $\theta^{(\alpha)}(l)$ and $\psi(l) \equiv \theta^{(S)} - \theta^{(R)}$ for a single induced-helical polymer, respectively. In the preceding section, the above quantities for a single polymer are derived as functions of the dimensionless tension τ. But these can be also regarded as functions of the normalized end-to-end distance l because there is a one-to-one relationship between τ and l. First we define $\theta_{network}^{(\alpha)}(\hat{\lambda})$ as

$$\theta_{network}^{(\alpha)}(\hat{\lambda}) \equiv \int \theta^{(\alpha)}(l)\, P(\boldsymbol{l})\, d\boldsymbol{l} \quad (19)$$

As in the case of the stress−strain relationship mentioned above, we have the affineness assumption and the three-chain approximation on the network. Equation 19 is finally given in the following form:

$$\theta_{network}^{(\alpha)}(\hat{\lambda}) \simeq \frac{1}{3}\left\{\theta^{(\alpha)}(\lambda l_{av}) + 2\theta^{(\alpha)}\left(\frac{l_{av}}{\lambda^{1/2}}\right)\right\} \quad (20)$$

Similarly, we have the explicit expression of $\psi_{network}(\hat{\lambda})$ in the following form:

$$\psi_{network}(\hat{\lambda}) \equiv \int \psi(l)\, P(\boldsymbol{l})\, d\boldsymbol{l} \simeq \frac{1}{3}\left\{\psi(\lambda l_{av}) + 2\psi\left(\frac{l_{av}}{\lambda^{1/2}}\right)\right\} \quad (21)$$

If the network is sufficiently transparent, this order parameter is propotional to the optical quantities such as ICD.

4. Results and Discussion

Before the discussion on the numerical results, we here introduce the enantiomeric excess *ee* as

$$ee \equiv \frac{c^{(S)} - c^{(R)}}{c^{(S)} + c^{(R)}} \quad (22)$$

to describe the chiral polarization of solutions. The possible range of *ee* is $-1 \le ee \le 1$. $ee = 1$ and $ee = -1$ correspond to the solutions of the chiral molecules in the (*S*)-form only and those of the chiral molecules in the (*R*)-form only, respectively. The condition $ee = 0$ corresponds to the solutions containing the chiral molecules in the (*S*)-form and those in the (*R*)-form equivalently (referred to as racemic form). In addition, we introduce the total molar concentration of the chiral molecules as $c \equiv c^{(S)} + c^{(R)}$. By using the above two quantities, the scaled concentrations of the α-type chiral molecules are rewritten as $\gamma_S = (1 + ee)\gamma/2$ and $\gamma_R = (1 - ee)\gamma/2$, respectively. γ is the scaled quantity for the total concentration of the chiral molecules and is defined as $\gamma \equiv k(T)c$.

We here explain the parameters used in the present numerical calculation. We choose $n = 100$ for the number of segments of each constituent chain in the network and $\sigma = 0.01$ for the helix initiation parameter. Since the value of κ of helices formed on induced-helical polymers remains unknown, we use the typical value of α-helices formed on homopolypeptides, i.e., $\kappa = 0.4$.

4.1. Networks in Solutions Containing One Type of Chiral Molecules. In this subsection, we study the simple case of solutions in which chiral molecules in either (*S*)- or (*R*)-form are dissolved ($ee = \pm 1$). Here, we can consider the case of $ee = 1$ without loss of generality.

We first present the typical numerical results for a single induced-helical polymer. Figure 4 shows (a) the (*S*)-type helix content $\theta^{(S)}$ and (b) the dimensionless tension τ as functions of the normalized end-to-end distance l at three values of the scaled concentration of the chiral molecules: $\gamma = 0.8$, 1.0, and 1.2. In the case of $ee = \pm 1$, the transition concentration of chiral molecules where free induced-helical polymers in a solution undergo the helix−coil transition is $\gamma = 1.0$ as reported by Tanaka.[4] Hence, the chosen three concentrations cover all the range of possible states of the polymers. When $ee = 1$, the helix content $\theta^{(S)}$ is equivalent to the chirality order parameter ψ. In Figure 4a, as the single polymer is stretched, the helix content

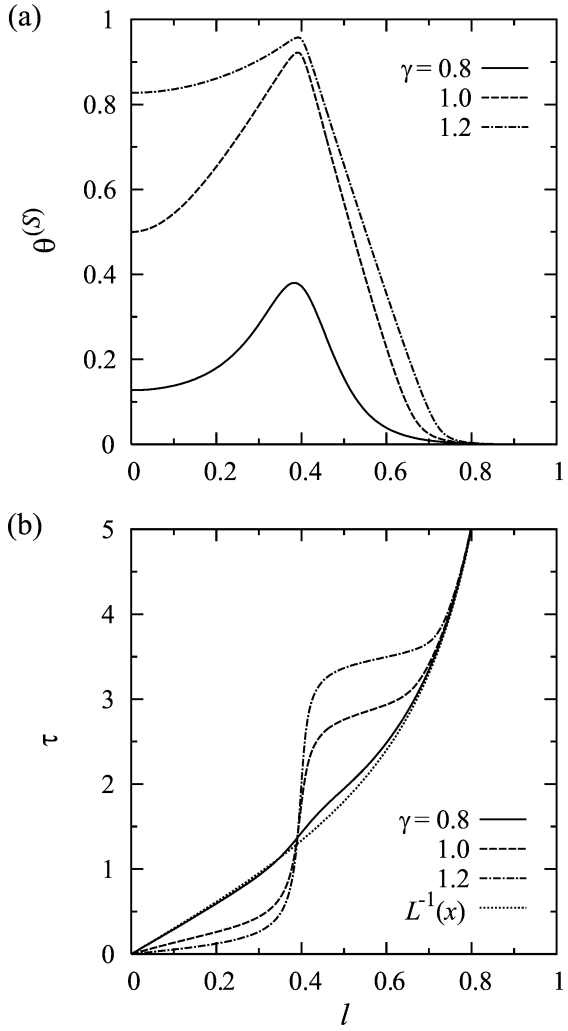

Figure 4. (a) The (*S*)-type helix content $\theta^{(S)}$ and (b) the dimensionless tension τ are plotted as functions of the normalized end-to-end distance l of a single chain for varying scaled concentration γ of the chiral molecules. Both figures correspond to $n = 100$, $\sigma = 0.01$, and $\kappa = 0.4$. In (b), the dotted line shows the inverse Langevin function $L^{-1}(x)$.

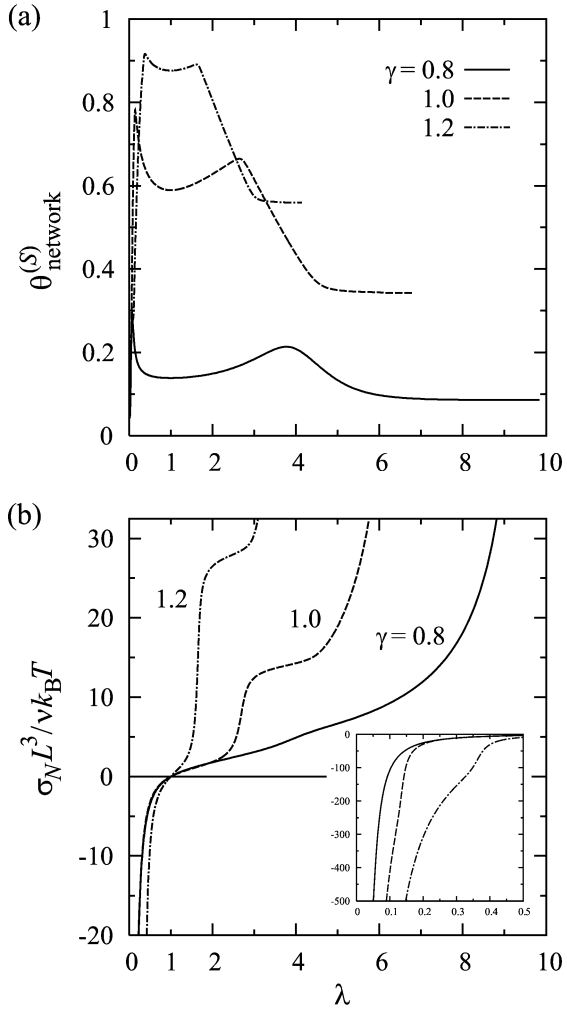

Figure 5. (a) The (*S*)-type helix content $\theta^{(S)}_{\text{network}}$ and (b) the dimensionless normal stress $\sigma_N L^3/\nu k_B T$ are plotted as functions of the strain factor λ of a cross-linked network for varying scaled concentration γ of the chiral molecules. Both figures correspond to $n = 100$, $\sigma = 0.01$, and $\kappa = 0.4$. In (a), we interpolate horizontal lines around states of the elongational limit because of the difficulty of the numerical calculation. In (b), the inset shows the expanded region with respect to the strain factor: $0 \le \lambda \le 0.5$.

first increases, then reaches a peak around $l = 0.4$, and finally decays toward 0. In addition, as the scaled concentration of the chiral molecules increases, the helix content at $l = 0$ and that at the peak increase together. The increase of the helix content in the low extension region ($l < 0.4$) is due to the competition between the entropy loss by the conformational constraint of the polymer and the energy gain by the formation of helices. On the other hand, the decay in the high extension region ($l > 0.4$) is due to the destruction of helical domains by overstretching the polymer. The value of $l = 0.4$ around which the profile shows the peak corresponds to the end-to-end distance of a perfectly helical chain ($\theta^{(S)} = 1$) because we choose $\kappa = 0.4$. In Figure 4b, the force−extension curves show two anomalous plateau regions and an abrupt jump at the boundary of these regions ($l \simeq 0.4$). As the scaled concentration of the chiral molecules increases, these features are made much clearer, and the profiles are far from the inverse Langevin function $L^{-1}(x)$, which is the force−extension curve of a normal random flight chain without helices. Compared with the behavior of the helix content, we can understand that the two plateau regions are relevant to the coexistence of helical and random coil domains, which is reminiscent of a first-order transition, and that the abrupt jump in the tension represents the onset of the destruction of induced helices.

We next present the numerical results for a network made by cross-linking induced-helical polymers discussed above. Figure 5 shows (a) the (*S*)-type helix content $\theta^{(S)}_{\text{network}}$ and (b) the dimensionless normal stress $\sigma_N L^3/\nu k_B T$ as functions of the strain factor λ of the network at three values of the scaled concentration of the chiral molecules mentioned before. When $ee = 1$, the helix content $\theta^{(S)}_{\text{network}}$ is equivalent to the chirality order parameter ψ_{network} and then is an experimentally measurable quantity. In Figure 5a, as the network is uniaxially elongated ($\lambda > 1$) or compressed ($\lambda < 1$), the helix content first increases, then reaches a peak, and finally decays toward a steady value. In addition, as the scaled concentration of the chiral molecules increases, the helix content in the natural state ($\lambda = 1$) increases. The appearance of the peaks is due to the elongation-induced formation and destruction of helices on the constituent polymers in the network. The peak which occurs at uniaxial compression is higher than that at uniaxial elongation for any concentration of the chiral molecules. The reason is as follows: the extension of two components of chains pointing toward *y*- and *z*-axes mainly contributes to uniaxial compression, whereas that of only one component of chains pointing toward *x*-axis mainly contributes to uniaxial elongation. Note that

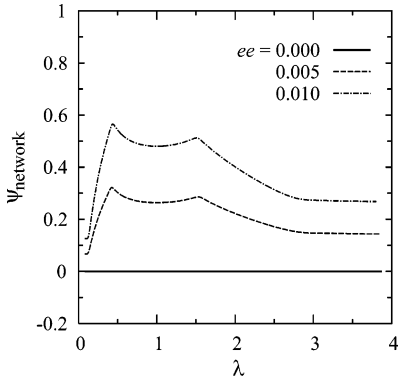

Figure 6. Chirality order parameter $\psi_{network}$ is plotted as a function of the strain factor λ for varying enantiomeric excess *ee* of solutions. The figure corresponds to $n = 100$, $\sigma = 0.01$, $\gamma = 3.0$, and $\kappa = 0.4$. We interpolate horizontal lines around states of the elongational limit.

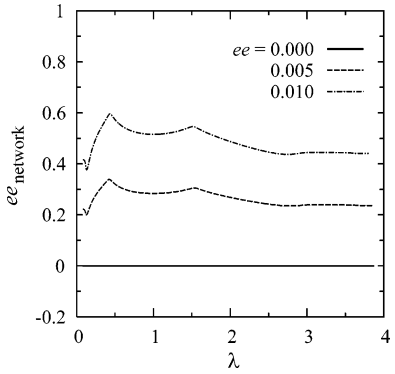

Figure 7. Enantiomeric excess $ee_{network}$ of the network is plotted as a function of the strain factor λ for varying enantiomeric excess *ee* of solutions. The figure corresponds to $n = 100$, $\sigma = 0.01$, $\gamma = 3.0$, and $\kappa = 0.4$. We interpolate horizontal lines around states of the elongational limit.

uniaxial compression is equivalent to biaxial elongation under the assumption that the volume of the network is conserved. In Figure 5b, the stress−strain curves have characteristic profiles different from sigmoidal ones observed for rubberlike materials made up of synthetic polymers without higher-order structures such as α-helices and β-sheets.[13,14] In both elongational and compressional cases, shoulders are observed in the strain regions where the helix content decreases. As the concentration of the chiral molecules increases, the shoulders are made much clearer. The shoulders mainly reflect the destruction of helices induced on an ensemble of chains in the network. The rapid divergence in the stress under large deformation is due to the finite extensibility of the constituent polymers in the network.

The networks made up of biopolymers such as homopolypeptides have been recently studied through theoretical, computational, and experimental approaches. Kutter and Terentjev[15] constructed a novel network model by combining the statistical theory of a single helix-forming polymer proposed by Buhot and Halperin[16] with a conventional network theory. Varshney and Carri[17] calculated elastic, conformational, and thermodynamic properties of a coarse-grained model chain which can undergo the helix−coil transition by using a Monte Carlo method based on the Wang−Landau sampling algorithm.[18] They combined the numerical results for the above single model chain with the three-chain model to investigate mechanical and conformational properties of the network made up of such helical polymers.[19,20] The relationship between the helix content and macroscopic deformation of the network independently calculated by Kutter and Terentjev[15] and Carri et al.[19,20] has almost similar profiles to the ones shown in Figure 5a although the molecular mechanism of helix formation is different. Courty et al.[21,22] later confirmed such relationship for a biopolymer network (gelatin gel) experimentally by combining a method for measuring the optical rotation, which is proportional to the helix content, with a stress−strain apparatus. The stress−strain relation calculated by Carri et al.[19,20] also has similar profiles to the ones shown in Figure 5b.

4.2. Networks in Solutions Containing Almost Racemic Chiral Molecules. In this subsection, we study the more interesting case of solutions in which chiral molecules in almost racemic form are dissolved ($ee \simeq 0$) and then discuss the possibility of optical resolution by macroscopically deforming the cross-linked network in such solutions. Figure 6 shows the chirality order parameter $\psi_{network}$ as a function of the strain factor λ of the network at three values of enantiomeric excess of solutions: $ee = 0.000$, 0.005, and 0.010. When $ee = 0$, chiral symmetry in the whole system is completely maintained. Therefore, any macroscopic deformation of the network leads to $\psi_{network} = 0$. This means that the network in the case of $ee = 0$ is always optically inactive. In contrast, when *ee* slightly deviates from 0, the small chiral symmetry breaking is largely amplified as the preferential adsorption of the major component of chiral molecules onto the constituent chains in the network, leading to finite chirality order parameter of the network even in the natural state. When the network is uniaxially elongated or compressed in the case of $ee \neq 0$, the chirality order parameter first increases, then reaches a peak, and finally decays toward a steady value.

Although the chirality order parameter is indeed an experimentally measurable quantity, the quantity is useless to discuss the optical resolution procedure. In order to describe the chiral polarization of the network itself, we here introduce the enantiomeric excess $ee_{network}$ of the network as

$$ee_{network} \equiv \frac{\theta^{(S)}_{network} - \theta^{(R)}_{network}}{\theta^{(S)}_{network} + \theta^{(R)}_{network}} \tag{23}$$

Figure 7 shows the enantiomeric excess $ee_{network}$ of the network as a function of the strain factor λ of the network at three values of enantiomeric excess of solutions mentioned before. When $ee = 0$, any macroscopic deformation of the network leads to $ee_{network} = 0$. In contrast, when *ee* slightly deviates from 0, the small chiral symmetry breaking is largely amplified as finite enantiomeric excess of the network as in the case with the chirality order parameter. For example, even in the natural states ($\lambda = 1$), $ee_{network} = 0.28$ in the case of $ee = 0.005$ (56 times that of the surrounding solution) and $ee_{network} = 0.52$ in the case of $ee = 0.010$ (52 times) as shown in Figure 7. In addition, when the network is uniaxially elongated or compressed in the case of $ee \neq 0$, the enantiomeric excess of the network shows a transient increase. An example of the simplest procedures as application of this principle to optical resolution is as follows: (1) swelling of the network in a solution with *ee* slightly deviated from 0; (2) macroscopic deformation of the network in the solution in order to preferentially adsorb the major component of chiral molecules onto the constituent chains in the network; (3) washing of the deformed network in a pure solvent in order to remove the chiral molecules attached on the constituent chains; (4) condensation of the solvent used for the washing process by evaporation of solvent molecules; (5) macroscopic deformation of the network in the condensed solution; (6) repetition of operations 3−5. The repetition of operations 3−5

results in separating almost racemic mixture of chiral molecules into optically pure species in principle.

5. Conclusion

In this paper, we have proposed a simple network model for chiral stimuli-responsive gels by a combination of the statistical theory of a single induced-helical polymer chain presented in our previous paper[6] and a conventional affine network theory in order to investigate mechanical and optical responses of such a network to macroscopic deformation. We have found that the stress−strain relation of the network in a solution of chiral molecules has characteristic profiles that are not observed in conventional networks made up of random-coil polymers without higher-order structures. We also have found that as the network is macroscopically deformed, the chirality order parameter shows a transient increase under appropriate conditions. Finally, we have discussed the possibility of optical resolution of chiral molecules in almost racemic form by using such network.

However, there are several important points to be improved in our present model. First, the swelling behavior of the network is basically determined by the competition between the elastic free energy of the network and the translational entropy of solvent molecules in the network. In the present study, we do not take into account the latter effect for simplicity. Hence, a variable L is not exactly a side length of a cubic network under swelling equilibrium states. In order to make the model more realistic, we need to properly add the translational entropy of the solvent molecules and of the chiral molecules in the network to the free energy of the whole system. Second, the affineness assumption does not generally hold for the networks made up of rigid chains such as helices. In the future studies, we need to reconstruct the present model on the basis of a network theory without affineness assumption, e.g., the phantom network theory first proposed by James and Guth.[23,24]

In this study, we kept the number of segments of each constituent chain in the network $n = 100$. We are very interested in the dependence of several physical quantities on the number of segments. From an experimental viewpoint, it is relatively easy to control the degree of polymerization (DP) of cross-linked chains in the network by stoichiometrically adding cross-linkers to the reacting system.[9] Another point of interest is how chiral external fields such as elliptically polarized light and circular-polarized light influence the network system in a solution of chiral molecules. Such external fields probably break the chiral symmetries of several variables such as σ, $k(T)$, and κ in our model. It is expected that such chiral symmetry breaking realizes optical resolution of exactly racemic mixture of chiral molecules by the procedure proposed in the preceding section. In our previous paper,[6] the effect of asymmetry in κ was already studied for a single induced-helical polymer system, and it was found that the stretching of the polymer can lead to optical resolution of the exactly racemic mixture.

These problems will be addressed in the future studies, together with the direct comparison between numerical and experimental results. We hope that both mechanical and optical properties of the chiral stimuli-responsive gels prepared by Goto et al.[9] will be measured by using experimental methods such as that devised by Courty et al.[21,22]

References and Notes

(1) Yashima, E.; Matsushima, T.; Okamoto, Y. *J. Am. Chem. Soc.* **1995**, *117*, 11596.
(2) Yashima, E.; Matsushima, T.; Okamoto, Y. *J. Am. Chem. Soc.* **1997**, *119*, 6345.
(3) Maeda, K.; Morino, K.; Okamoto, Y.; Sato, T.; Yashima, E. *J. Am. Chem. Soc.* **2004**, *126*, 4329.
(4) Tanaka, F. *Macromolecules* **2004**, *37*, 605.
(5) D'Orsogna, M. R.; Chou, T. *Phys. Rev. E* **2004**, *69*, 021805.
(6) Toda, M.; Tanaka, F. *Macromolecules* **2005**, *38*, 561.
(7) Smith, S. B.; Finzi, L.; Bustamante, C. *Science* **1992**, *258*, 1122.
(8) Perkins, T. T.; Quake, S. R.; Smith, D. E.; Chu, S. *Science* **1994**, *264*, 822.
(9) Goto, H.; Zhang, H. Q.; Yashima, E. *J. Am. Chem. Soc.* **2003**, *125*, 2516.
(10) Zimm, B. H.; Bragg, J. K. *J. Chem. Phys.* **1959**, *31*, 526.
(11) Poland, D.; Scheraga, H. A. *Theory of Helix−Coil Transitions in Biopolymers*; Academic Press: New York, 1970.
(12) Kuhn, W. *Kolloid Z.* **1936**, *76*, 258.
(13) James, H. M.; Guth, E. *J. Chem. Phys.* **1943**, *11*, 455.
(14) Treloar, L. R. G. *The Physics of Rubber Elasticity*; Clarendon Press: Oxford, UK, 1975.
(15) Kutter, S.; Terentjev, E. M. *Eur. Phys. J. E* **2002**, *8*, 539.
(16) Buhot, A.; Halperin, A. *Macromolecules* **2002**, *35*, 3238.
(17) Varshney, V.; Carri, G. A. *Macromolecules* **2005**, *38*, 780.
(18) Wang, F.; Landau, D. P. *Phys. Rev. Lett.* **2001**, *86*, 2050.
(19) Carri, G. A.; Batman, R.; Varshney, V.; Dirama, T. E. *Polymer* **2005**, *46*, 3809.
(20) Batman, R.; Carri, G. A. *Polymer* **2005**, *46*, 10128.
(21) Courty, S.; Gornall, J. L.; Terentjev, E. M. *Proc. Natl. Acad. Sci. U.S.A.* **2005**, *102*, 13457.
(22) Courty, S.; Gornall, J. L.; Terentjev, E. M. *Biophys. J.* **2006**, *90*, 1019.
(23) James, H. M. *J. Chem. Phys.* **1947**, *15*, 651.
(24) James, H. M.; Guth, E. *J. Chem. Phys.* **1947**, *15*, 669.

MA070759W